International Immunology, Vol. 22, No. 5, pp. 375–386
doi:10.1093/intimm/dxq017
Advance Access publication 9 March 2010

© The Japanese Society for Immunology. 2010. All rights reserved.
For permissions, please e-mail: journals.permissions@oxfordjournals.org

Zinc suppresses T_h17 development via inhibition of STAT3 activation

Chika Kitabayashi[1,*], Toshiyuki Fukada[2,3], Minoru Kanamoto[1], Wakana Ohashi[4,7], Shintaro Hojyo[2,3], Toru Atsumi[1], Naoko Ueda[1], Ichiro Azuma[5], Hiroshi Hirota[4,6], Masaaki Murakami[1,*] and **Toshio Hirano[1,2]**

[1]Laboratory of Developmental Immunology, JST-CREST, Graduate School of Frontier Biosciences, Graduate School of Medicine and WPI Immunology Frontier Research Center, Osaka University, Osaka 565-0871, Japan
[2]Laboratory of Cytokine Signaling, RIKEN Research Center for Allergy and Immunology, Yokohama 230-0045, Japan
[3]Department of Allergy and Immunology, Osaka University Graduate School of Medicine, Osaka University, Osaka 565-0871, Japan
[4]RIKEN Genomic Sciences Center, 1-7-22 Suehiro, Tsurumi, Yokohama, Kanagawa 230-0045, Japan
[5]Hokkaido Pharmaceutical University, 7-1 Katsuraoka-cho, Otaru, Hokkaido 047-0264, Japan

[6]Present address: Antibiotics Laboratory, RIKEN Advanced Science Institute, 2-1 Hirosawa, Wako, Saitama 351-0198, Japan
[7]Present address: Laboratory of Cytokine Signaling, RIKEN Research Center for Allergy and Immunology, Yokohama 230-0045, Japan

*These authors equally contributed to this study.

Correspondence to: T. Hirano; E-mail: hirano@molonc.med.osaka-u.ac.jp

Transmitting editor: S. Koyasu

Received 18 November 2009, *accepted* 2 February 2010

Abstract

Zinc (Zn) is an essential trace metal required by many enzymes and transcription factors for their activity or the maintenance of their structure. Zn has a variety of effects in the immune responses and inflammation, although it has not been well known how Zn affects these reactions on the molecular basis. We here showed that Zn suppresses T_h17-mediated autoimmune diseases at lest in part by inhibiting the development of T_h17 cells via attenuating STAT3 activation. In mice injected with type II collagen to induce arthritis, Zn treatment inhibited T_h17 cell development. IL-6-mediated activation of STAT3 and *in vitro* T_h17 cell development were all suppressed by Zn. Importantly, Zn binding changed the α-helical secondary structure of STAT3, disrupting the association of STAT3 with JAK2 kinase and with a phospho-peptide that included a STAT3-binding motif from the IL-6 signal transducer gp130. Thus, we conclude that Zn suppresses STAT3 activation, which is a critical step for T_h17 development.

Keywords: autoimmune disease, STAT3, T_h17, Zinc

Introduction

Zn, one of the essential trace elements (1–4), is required by many enzymes and transcription factors for their activity or the maintenance of their structure. Zn has a variety of effects in the immune system (3, 5, 6). It was reported that mature $CD4^+$ and $CD8^+$ T cells are quite resistant to Zn deficiency and survived well in the otherwise atrophying thymus (7). Interestingly, Zn deficiency in an experimental mouse model causes an imbalance between T_h1 and T_h2 functions in periphery. Production of IFN-gamma and IL-2 (products of T_h1) is decreased, whereas production of IL-4, IL-6 and IL-10 (products of T_h2) is not affected even during Zn deficiency (8). The relationships between Zn and autoimmune diseases have been described previously (9, 10). Such interactions include altered serum Zn concentrations in many chronic autoimmune diseases and inhibition of several animal models of these diseases by Zn supplementation. For example, it is reported that the dextran sulfate sodium-induced colitis and diabetes induced by multiple low does of streptozotocin are suppressed by Zn administration (11–13). However, a molecular mechanism how Zn suppresses the diseases has not been demonstrated yet.

Because cytokines and Toll-like receptor (TLR) stimulation affect the expression profiles of Zn transporters (14–16), we hypothesized that proteins involved in inflammation and

FEATURED ARTICLE

Downloaded from https://academic.oup.com/intimm/article/22/5/375/730670 by guest on 21 October 2022

autoimmune diseases, such as STAT3, may be targets of Zn signaling. We were particularly interested in how Zn affects T_h17 cells, because T_h17 cell development is controlled by IL-6-induced STAT3 activation (17–21), although it is well known that STAT3 plays a role in a lot of biological reactions and its activation state is sophisticatedly regulated (22, 23). Moreover, although classification of $CD4^+$ T cells into T_h1 and T_h2 cells has provided a framework for understanding the roles of various $CD4^+$ T-cell subtypes in the development of autoimmune diseases (24–26), recent studies have identified T_h17 cells as a previously unknown arm of the $CD4^+$ T-cell effector response. These cells secrete several pro-inflammatory cytokines, including IL-17A (18, 21, 27–29), deficiency of which in mice results in resistance to such autoimmune diseases as collagen-induced arthritis (CIA), experimental autoimmune encephalomyelitis (EAE) and the arthritis disorders that develop in F759, SKG and IL-1 receptor antagonist-deficient mice (18, 30–33), although the relationship between Zn and T_h17 development has not been investigated yet.

Our group and others showed that Zn functions as an intracellular signaling molecule by demonstrating that a variety of extracellular stimuli affect the intracellular levels of free Zn (34–36). For example, LPS stimulation of TLRs decreases intracellular-free Zn levels in a manner that is dependent on altered Zn transporter expression in dendritic cells (15), whereas Fc epsilon receptor-1 (FcεR-1) stimulation rapidly induces Zn release from perinuclear regions of mast cells, a process referred to as the 'Zn wave' (37). Interestingly, FcεR-1-induced translocation of protein kinase C to the plasma membrane and the subsequent nuclear factor κB-mediated cytokine expression in mast cells involves the Zn transporter Znt5/Slc30a5 (38). In addition, the expression of the Zn transporter Zip6/Slc39a6/Liv1 is dependent on STAT3 and is required for the nuclear localization of the Zn-finger transcription factor Snail (14). Another Zn transporter, Zip13/Slc39a13, is required for transforming growth factor (TGF)-β/BMP signaling, an effect that is mediated by Smad nuclear localization (39). In *Caenorhabditis elegans*, the Zn transporter CDF1, a nematode ZnT1 ortholog, positively regulates Ras–Raf–Mek–extracellular signal-regulated kinase (ERK) signal transduction by promoting Zn efflux and reducing the cytosolic Zn concentration (40). These studies raise the possibility that Zn may directly regulate the structures of target proteins to affect their biological activities, an effect that has not yet been demonstrated.

The present study shows that Zn directly suppresses STAT3 activation, which is a critical step in T_h17 cell development, and suggested that STAT3 might be a target of Zn signaling in T cells.

Methods

Mice

C57BL/6 mice were purchased from CLEA Japan or Japan SLC (Tokyo, Japan). All mice were maintained under specific pathogen-free conditions according to the protocols of the Osaka University Medical School and RIKEN Research Center for Allergy and Immunology (RCAI). All animal experiments were performed following the guidelines of the Institutional Animal Care and Use Committees of the Graduate School of Frontier Bioscience (Graduate School of Medicine, Osaka University) and the RIKEN RCAI.

CIA development

CIA was induced in C57BL/6 mice (Japan SLC) essentially as previously described (41). Mice were injected intradermally in their back with 200 μg of chicken type II collagen plus 250 μg of *Mycobacterium bovis* Bacillus Calmette-Guérin cell wall skeleton (BCG-CWS) emulsified in CFA. Three weeks after the initial injection, a booster injection containing 200 μg of chicken type II collagen plus 250 μg of BCG-CWS emulsified in CFA was given intra-dermally in the base of the tail. Clinical arthritis activity was evaluated every 3 days after the second immunization for 21 days. Arthritis severity in the metacarpophalangeal, wrist, metatarsophalangeal and ankle joints was scored using the following scale: 0 = no arthritis, 1 = small degree of arthritis, 2 = mild swelling, 3 = moderate swelling, and 4 = severe swelling and non-weight bearing. The arthritic score was the sum of the scores from all the involved joints.

Induction of EAE. EAE was induced and scored as described previously (42).

Cell culture

The RAW246.7 mouse myeloid leukemia cell line, human Jurkat T-cell line, human fibroblast cell line and 293T-G133 cells (43), which produce granulocyte colony-stimulating factor (CSF) receptor–gp130 receptor protein chimeras, were cultured in RPMI-1640 medium supplemented with 10% fetal bovine serum (FBS). Mouse ProB Baf/B03 cells were maintained in RPMI-1640 medium supplemented with 10% FBS and 10% conditioned medium from WEHI3B cells as a source of IL-3.

Transfection

Cells were transfected using Lipofectamine 2000 (Invitrogen), according to the supplier's protocol. Typically, 10 μg of expression plasmid, pEFBOS or pEFBOS encoding HA-tagged JAK1 was used. Cells were incubated with DNA–lipid complexes for 24 h and subjected to other biochemical analyses.

Immunoblotting

Cells were serum starved for 12 h, stimulated with LPS or the indicated cytokines (50 ng ml^{-1}) for the indicated period of time and suspended in 1 ml of 1% NP-40 buffer [1% NP-40, 20 mM Tris–HCl (pH 7.4), 150 mM NaCl, 5 μg ml^{-1} aprotinin, 0.1 mM phenylmethylsulfonyl fluoride and 1 mM Na_3VO_4). In some experiments, cells were treated with the indicated final concentrations of $ZnSO_4$ and pyrithione at 37°C for the indicated period of time before cytokine stimulation. A NativePAGE Novex Bis-Tris Gel System (Invitrogen) was used according to the supplier's manual. Proteins on the blotted membrane were probed with the indicated antibodies and detected using enhanced chemiluminescence (PerkinElmer Life Science). Anti-ERK1/2, anti-phospho-ERK1/2 and anti-JAK1 antibodies were obtained from BD

Downloaded from https://academic.oup.com/intimm/article/22/5/375/730670 by guest on 21 October 2022

Transduction Laboratories. Tyrosine-phosphorylated proteins were detected with 4G10 antibodies (Upstate). Antibodies specific for phospho-Tyr1022/1023-JAK1, JAK2, phospho-Tyr1007/1008-JAK2, STAT3 and phospho-Tyr705-STAT3 were purchased from Cell Signaling Technology.

Immunoprecipitation

Cell lysates were suspended in 1 ml of 1% NP-40 buffer and mixed with 20 μl of protein A–Sepharose or protein G–Sepharose (Pharmacia) and 1 μg of each antibody, followed by incubation for 6 h at 4°C. The immunoprecipitates were eluted with SDS–PAGE loading buffer, separated by SDS–PAGE and transferred to a PVDF membrane.

In vitro binding assay

The peptide-binding assay was performed using biotinylated peptides representing gp130 (VVHSG-pY^{767}RHQVPS and VVHSGY^{767}RHQVPS), which were purchased from Toray Research Center. The peptides (5 μg) were incubated with 30 μl of streptavidin–Sepharose (Pharmacia) for 2 h at 4°C. The beads were washed three times with 20 mM Tris–HCl (pH 7.4) and then incubated with 0.1 μg of recombinant recombinant STAT3 (rSTAT3) (Active Motif) for 3 h at 4°C. rSTAT3 was treated with $ZnSO_4$ for 2 h at 4°C. The complexes were separated using SDS–PAGE and blotted with anti-STAT3 antibodies. GST-JAK2 (Active Motif) was used to assess the JAK2–STAT3 interaction. GST-JAK2 (0.1 μg) was incubated with 30 μl of glutathione–Sepharose 4B (Pharmacia) at 4°C for 2 h, and the JAK2-bound beads were incubated with rSTAT3 for 3 h at 4°C.

Precipitation assay using Zn immobilized on beads

Immobilized metal affinity chromatography (IMAC)-select affinity beads were obtained from Sigma. Zn was immobilized on the IMAC-select affinity beads by rotating equal volumes of IMAC-select affinity beads with $ZnSO_4$ (50 mM) for 1 h at 4°C. The beads were then washed five times with 1% NP-40 buffer and used to precipitate rSTAT3 from solution or RAW246.7 cell lysates, as indicated. The beads (30 μl) were added to either rSTAT3 solution or whole-cell lysates and rotated for 2 h at 4°C. They were then washed four times with 1% NP-40 lysis buffer and precipitated. The pellet was re-suspended in SDS–PAGE loading buffer for further immunoblotting.

DNA pull-down assay

DNA pull-down assays were performed as described previously (44). Biotinylated double-stranded DNA probes for the mouse Socs3/STAT-binding element (SBE), derived from the mouse *Socs3* promoter (45), were as follows: mSocs3/SBE-F, biotin 3′-CAGTTCCAGGAATCGGGGGGC-5′ and mSOCS3/SBE-R, biotin 3′-GCCCCCCGATTCCTGGAACTG-5′.

In vitro kinase assay

The 293T-G133 cells were transfected with either pEFBOS-HA-JAK1 or empty pEFBOS expression plasmid, followed by stimulation with G-CSF to activate JAK1. Cells were suspended in 1 ml of lysis buffer [0.5% NP-40, 50 mM Tris–HCl (pH 7.4), 250 mM NaCl, 1 mM sodium vanadate and protease inhibitors]. Lysates were cleared by centrifugation, and 500 μg of each lysate was mixed with 4 μl of anti-HA antibody solution (clone 3F10, Roche) and 30 μl of protein G–Sepharose (Pharmacia). After a 4-h incubation at 4°C, the beads were washed three times with 0.5 ml of lysis buffer in the absence of protease inhibitors and three times with 0.5 ml of kinase buffer [60 mM HEPES–NaOH (pH 7.5), 3 mM $MgCl_2$ and 3 mM $MnCl_2$]. GST-JAK2 was used as JAK2 in these experiments. rSTAT3 or poly-AEKY (Sigma) was used as the substrate for the JAK kinases. The kinase reaction was performed by incubating the JAK proteins in 50 μl of the kinase buffer containing 1 mM ATP, 1.2 mM dithiothreitol and 50 ng of rSTAT3 or 1 μg of poly-AEKY for 30 min at 30°C. The reactions were stopped by the addition of Laemmli's SDS loading buffer, and the reaction products were subjected to SDS–PAGE, followed by immunoblotting with antibodies specific for individual tyrosyl-phosphorylated proteins, as indicated.

Real-time PCR

SYBR Green PCR Master Mix (Applied Biosystems) and a GeneAmp 7000 Sequence Detection System (Applied Biosystems) were used for quantitative PCRs as described previously (15). Transcript levels were normalized to those of the gene encoding glyceraldehyde-3-phosphate dehydrogenase (*Gapdh*). Primer sequences were as follows: mouse *Socs3*—CCCAAGGCCGGAGATTTC and GGAGCCAGCGTGGATCTG, mouse *Egr1*—TAGCAGCAGCAGCACCAG and GGCTGGGATAACTCGTCTCC and mouse *Gapdh*—AGCTGAACGGGAAGCTCACT and TGAAGTCGCAGGAGACAACC.

Circular dichroism spectroscopy

CD measurements of STAT3 under different solvent conditions were performed using a Jasco J-820 CD spectropolarimeter equipped with a Peltier temperature control unit. All CD spectra were recorded in a cuvette with a path length of 1 mm and a protein concentration of 1 μM. The CD spectrum was taken as the average of three successive spectra. Recombinant Flag-tagged mouse STAT3 was prepared using a silkworm–baculovirus protein expression system (Katakura Industries Co., Saitama, Japan).

Enzyme-linked immunosorbent assay

IFN-γ, IL-4 and IL-17A levels in serum or cell culture supernatant were determined using ELISA Kits (BD Biosciences or eBiosciences).

Intracellular staining

In vitro assay. The recommended amount of GolgiPlug (BD Biosciences) was added to the culture, which is stimulated with PMA (500 ng ml^{-1}) and ionomycine (500 ng ml^{-1}) for 6 h. Cells were stained with PE-Cy7-conjugated anti-CD4 antibodies and biotin-conjugated anti-CD19, anti-NK1.1 and anti-MHC class II antibodies (eBiosciences), followed by streptavidin–Pacific Blue treatment. Next, the cells were fixed and permeabilized according to the manufacturer's directions (BD Biosciences) and stained with FITC-conjugated anti-Foxp3 and PE-conjugated anti-IL-17A (eBiosciences) antibodies (eBiosciences). Data were acquired on a CyAn flow cytometer and analyzed with FlowJo software.

Downloaded from https://academic.oup.com/intimm/article/22/5/375/730670 by guest on 21 October 2022

In vivo assay. T cells from lymph nodes were stimulated in plates coated with anti-CD3 antibodies (20 μg ml^{-1}) and anti-CD28 antibodies (10 μg ml^{-1}) for 6 h. The recommended amount of GolgiPlug was added to the culture at the beginning of the incubation. The resulting cells were stained with allophycoerthrin (APC)-conjugated anti-CD44 (eBiosciences), PE-Cy7-conjugated anti-CD4 and biotin-conjugated anti-CD19, anti-NK1.1 and anti-MHC class II antibodies followed by streptavidin–Pacific Blue treatment. The cells were then fixed and permeabilized with a Cytofix/Cytoperm Plus Fixation/Permeabilization Kit (BD Biosciences) and stained with PE-conjugated anti-IL-17A (eBiosciences) and FITC-conjugated Foxp3 antibodies (eBiosciences). Data were acquired on a CyAn flow cytometer and analyzed with Summit software.

Detection of phospho-STAT3

In vitro assay. The lymph nodes and spleens from wild-type mice were harvested and the T-cell population was enriched using an nylon wool column. Incubations were performed with 2×10^6 cells in 100 μM $ZnSO_4$ for 30 min and 10 ng ml^{-1} IL-6 for 5 min. The cells were fixed immediately with Lyse/Fix buffer (BD Biosciences), permeabilized with Perm Buffer III (BD Biosciences) and stained with FITC-conjugated anti-CD19 and anti-MHC class II, PE-Cy5-conjugated anti-CD4, APC-conjugated anti-CD8 and PE-conjugated anti-Stat3(pY705) antibodies (BD Biosciences). Data were acquired on an FACSCalibur system (BD Biosciences) and analyzed with FlowJo software.

In vivo assay. Zn-treated and control mice were injected intravenously with 20 ng of IL-6. After 15 min, mice were sacrificed and the spleens were harvested. Single-cell suspensions from the spleen samples were fixed immediately with Lyse/Fix buffer, permeabilized with Perm Buffer III and stained with FITC-conjugated anti-CD19 and anti-MHC class II, PE-Cy5-conjugated anti-CD4, APC-conjugated CD8 and PE-conjugated anti-Stat3(pY705) antibodies. Data were acquired on an FACSCalibur system and analyzed with FlowJo software.

Induction of T_h1 and T_h17 cells

Lymph nodes and spleens from wild-type mice were harvested and $CD25^-CD44^{lo}$ naive $CD4^+$ T cells were sorted using a Moflo cell sorter (Beckman Coulter). The purity of the T-cell samples was consistently >99%. The cells were co-cultured for 4 days with bone marrow-derived dendritic cells plus anti-CD3 antibodies (1 μg ml^{-1}) in the presence of rmIL-12 (5 ng ml^{-1}; PeproTech) for T_h1 cells or in the presence of IL-6 (500 ng ml^{-1}) and rhTGF-β (5 ng ml^{-1}; PeproTech) for T_h17 cells.

Statistical analysis

Student's *t*-tests (two tailed) were used for statistical comparisons of two groups.

Results

Zn inhibits the development of CIA and T_h17 cell development in vivo

To induce T_h17 cell development *in vivo*, we employed the mouse model of T_h17 cell-mediated collagen induced arthritis (CIA), which is known to be dependent on both IL-6 and IL-17A (Supplementary Figure S1 is available at *International Immunology* Online) (41,46). As expected, CIA development was suppressed significantly when 3000 p.p.m. Zn was added to the animals' drinking water (Fig. 1A). We also showed that another T_h17 cell-mediated autoimmune disease, experimental autoimmune encephalomyelitis (EAE), was inhibited by the same Zn treatment (Fig. 1B). There were several reports using drinking water containing 2000–4000 p.p.m. Zn for the *in vivo* experiments (47–49). We confirmed that administering 3000 p.p.m. Zn for 2 months did not alter the sizes of various lymph node and spleen immune cell populations, including those of $CD4^+$ T cells, $CD8^+$ T cells, B cells, NK cells, $CD11c^+$ cells and $CD11b^+$ cells (Supplementary Figure S2 is available at *International Immunology* Online). Additionally, body weight of the mice having 3000 p.p.m. Zn was not changed comparing to that of control animals (data not shown). In fact, sera from mice that received drinking water containing 3000 p.p.m. Zn contained ~29 μM Zn, whereas the concentration in sera from control mice was ~15 μM (Supplementary Figure S3 is available at *International Immunology* Online). Zn (29 μM) is much lower than a toxic range. These data strongly suggested that mice having a drinking water with 3000 p.p.m. of Zn should have the normal immune responses. To confirm this idea, pathogenic T_h17 cells were transferred to mice that received drinking water supplemented with 3000 p.p.m. Zn for over 1 month before the experiments. The development of EAE was similar in Zn-treated and control mice (Fig. 1C). These results demonstrated that mice that were given drinking water supplemented with 3000 p.p.m. Zn showed normal T_h17 cell-mediated immune responses including activation of T_h17 cells and induction of inflammations, when the pathogenic T_h17 cells were existed. These results strongly suggested that Zn does not affect the immune responses after the processes of pathogenic T-cell development but inhibits T_h17-cell development from naive $CD4^+$ T cells. Therefore, we hypothesized that Zn suppresses T_h17-cell development during the induction of CIA, which is dependent on the IL-6–STAT3-signaling pathway. To test this possibility, we examined the serum concentrations of T cell-derived cytokines, including IFN-γ, IL-4 and IL-17A, after the first and second immunizations used to induce CIA. Zn treatment decreased the serum concentrations of IL-17A, a pro-inflammatory cytokine produced by T_h17 cells, whereas IFN-γ concentrations were similar in sera collected from mice supplied either Zn-containing or control water (Fig. 1D). On the other hand, IL-4 was not detected after the immunizations (data not shown). Consistent with these results, *ex vivo* experiments showed that Zn treatment suppressed IL-17A but not IFN-γ expression after T-cell activation (Fig. 1E), whereas IL-4 was not detected (data not shown). Moreover, we showed that the percentages and absolute numbers of T_h17 cells decreased in regional lymph nodes after Zn supplementation, whereas those of regulatory T (Treg) cells and T_h1 cells were not markedly affected (Fig. 1F and G). Importantly, Zn treatment inhibited STAT3 activation in $CD4^+$ T cells after *in vivo* IL-6 treatment (Fig. 1H). Taken together, these results showed that Zn supplementation contributed to the suppression of T_h17-cell development from naive $CD4^+$ T cells

Downloaded from https://academic.oup.com/intimm/article/22/5/375/730670 by guest on 21 October 2022

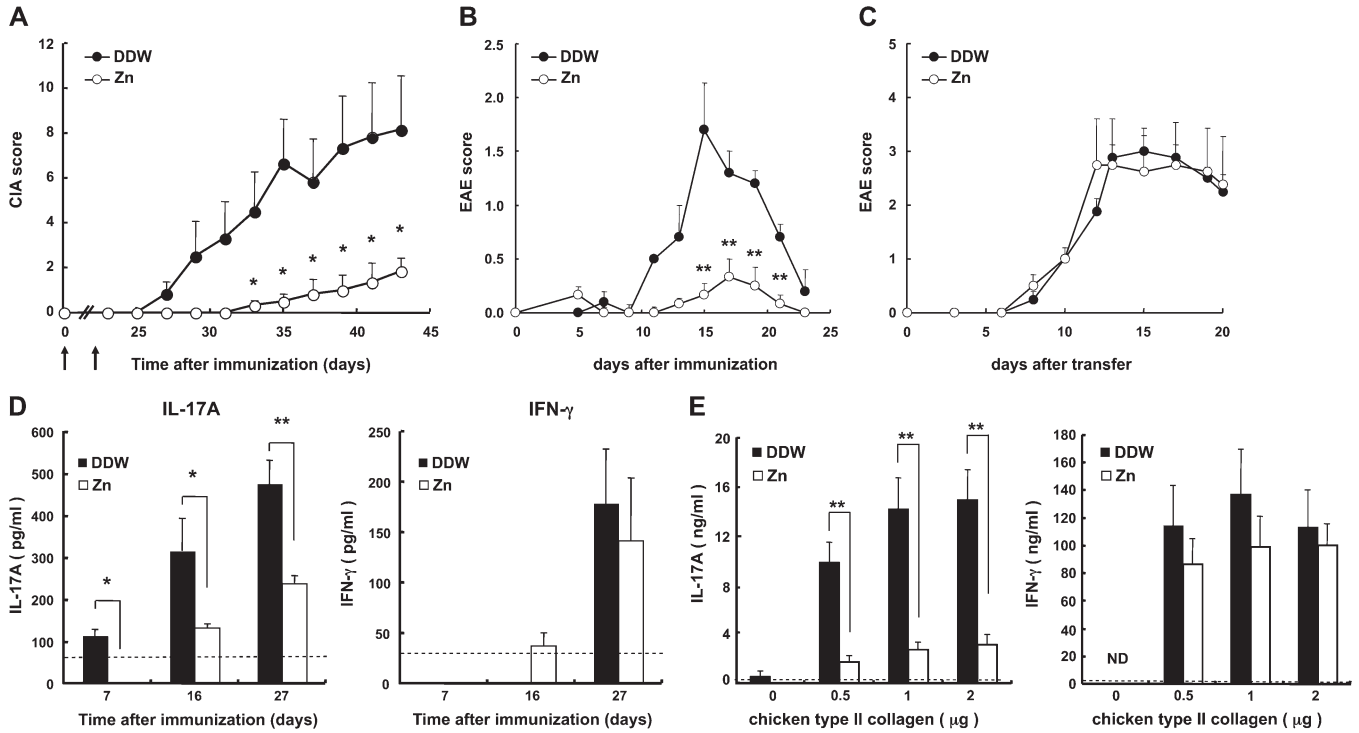

Fig. 1. Zn inhibited the development of CIA and T_h17 cells *in vivo*. DDW, an ultrapure water treated by distillation plus Barnstead ULTROpure. (A) C57BL/6 mice were given drinking water supplemented with Zn (3000 p.p.m., $n = 6$) or regular drinking water ($n = 6$) for at least 30 days. The mice were then injected subcutaneously with chicken type II collagen plus BCG-CWS with CFA (arrows: Days 0 and 21). CIA development was suppressed significantly in Zn-treated mice compared with control animals ($P = 0.043$, 0.011, 0.034, 0.026, 0.031 and 0.028 for Days 33, 35, 37, 39, 41 and 43, respectively). (B) C57BL/6 mice were given drinking water supplemented with Zn (3000 p.p.m., $n = 6$) or regular drinking water ($n = 5$) for at least 30 days. The mice were then injected subcutaneously with MOG (35–55) peptide (synthesized by Sigma) in CFA (Sigma–Aldrich) at the base of the tail on Day 0 followed by intravenous injection of pertussis toxin (List Biological Laboratories) on Days 0 and 2. EAE development was suppressed significantly in Zn-treated mice compared with control animals ($P = 0.023$, 0.0046, 0.0019, and 0.0020 for Days 15, 17, 19, and 21, respectively). (C) C57BL/6 mice were given drinking water supplemented with Zn (3000 p.p.m., $n = 4$) or regular drinking water ($n = 4$) for at least 30 days. The mice were intravenously injected with T_h17 cells from WT mice with EAE. The clinical EAE scores of C57BL/6 mice given drinking water supplemented with Zn (open circles, $n = 4$) were determined as described in the Methods and compared with those with regular drinking water (closed circles, $n = 4$). (D) C57BL/6 mice were given drinking water supplemented with Zn (IL-17A: $n = 10$, 10 and 31 for Days 7, 16 and 27, respectively; IFN-γ: $n = 4$, 4 and 16 for Days 7, 16 and 27, respectively) or regular drinking water (IL-17A: $n = 9$, 10 and 34 for Days 7, 16 and 27, respectively; IFN-γ: $n = 4$, 4 and 24 for Days 7, 16 and 27, respectively) for at least 30 days. CIA was then induced. Sera were collected on the indicated days after CIA induction and the IL-17A and IFN-γ concentrations were measured using ELISAs. Serum IL-17A concentrations were significantly lower in Zn-treated mice compared with control mice on Days 7, 16 and 27 ($P = 0.013$, 0.032 and 0.00071, respectively). Serum IFN-γ concentrations were not significantly affected. The dotted lines denote the thresholds of detection (62.5 pg ml^{-1} and 31.25 pg ml^{-1} for IL-17A and IFN-γ, respectively). (E) Single-cell suspensions made from the inguinal lymph nodes of mice 6 days after the second immunization were cultured with the indicated amount of chicken type II collagen. On Day 27 after the first immunization, IL-17A concentrations were lower in the culture media containing cells from Zn-treated mice compared with control samples ($P = 0.001$, 0.0019 and 0.0011 for 0.5, 1 and 2 μg of chicken type II collagen, respectively). The dotted lines denote the threshold of detection. (F) The percentages and numbers of T_h17 cells ($CD4^+CD44^{hi}IL\text{-}17A^+$) and Treg cells ($CD4^+CD44^{hi}Foxp3^+$) were examined in the inguinal lymph nodes of mice 6 days after the second immunization. The percentage and number of T_h17 cells ($CD4^+CD44^{hi}IL\text{-}17A^+$), but not those of Treg cells ($CD4^+CD44^{hi}Foxp3^+$), decreased in Zn-treated mice compared with control animals ($P = 0.019$ and 0.044 for the percentage and number, respectively). (G) The percentages and numbers of T_h1 cells ($CD4^+CD44^{hi}IFN\text{-}\gamma^+$) were examined in the inguinal lymph nodes of mice 6 days after the second immunization. The percentage and number of T_h1 cells ($CD4^+CD44^{hi}IFN\text{-}\gamma^+$) were not markedly affected ($P = 0.27$ and 0.76 for the percentage and number, respectively). (H) C57BL/6 mice were given drinking water supplemented with Zn (3000 p.p.m., $n = 12$) or regular drinking water ($n = 9$) for at least 30 days. IL-6 (20 ng per mouse) was intravenously injected and 15 min later the spleen of each mouse was collected. STAT3 phosphorylation in $CD4^+$ T cells—assessed using intracellular staining—was lower in Zn-treated mice compared with control mice ($P = 0.0081$). *P* values were calculated using Student's t-test (*$P < 0.05$, **$P < 0.01$). n.s., not detected.

in vivo. Moreover, the data suggested that Zn suppresses T_h17-cell development by inhibiting the IL-6–STAT3-signaling axis in naive $CD4^+$ T cells followed by inhibition of CIA development.

Zn inhibits the development of T_h17 cells in vitro

To eliminate the effects of other cell populations after Zn treatment, we employed an *in vitro* system in which T_h17-cell development was induced in the presence or absence of Zn. Because preliminary experiments showed that culture medium containing <100 μM of $ZnSO_4$ did not have a marked effect on $CD4^+$ T-cell viability (Supplementary Figure S4 is available at *International Immunology* Online), we used 50 μM $ZnSO_4$ for the subsequent *in vitro* experiments. Zn treatment significantly inhibited T_h17-cell development *in vitro*, whereas the number of Foxp3-expressing cells increased (Fig. 2A). Expression levels of Foxp3, however, were significantly low compared with those observed in normal Treg

Downloaded from https://academic.oup.com/intimm/article/22/5/375/730670 by guest on 21 October 2022

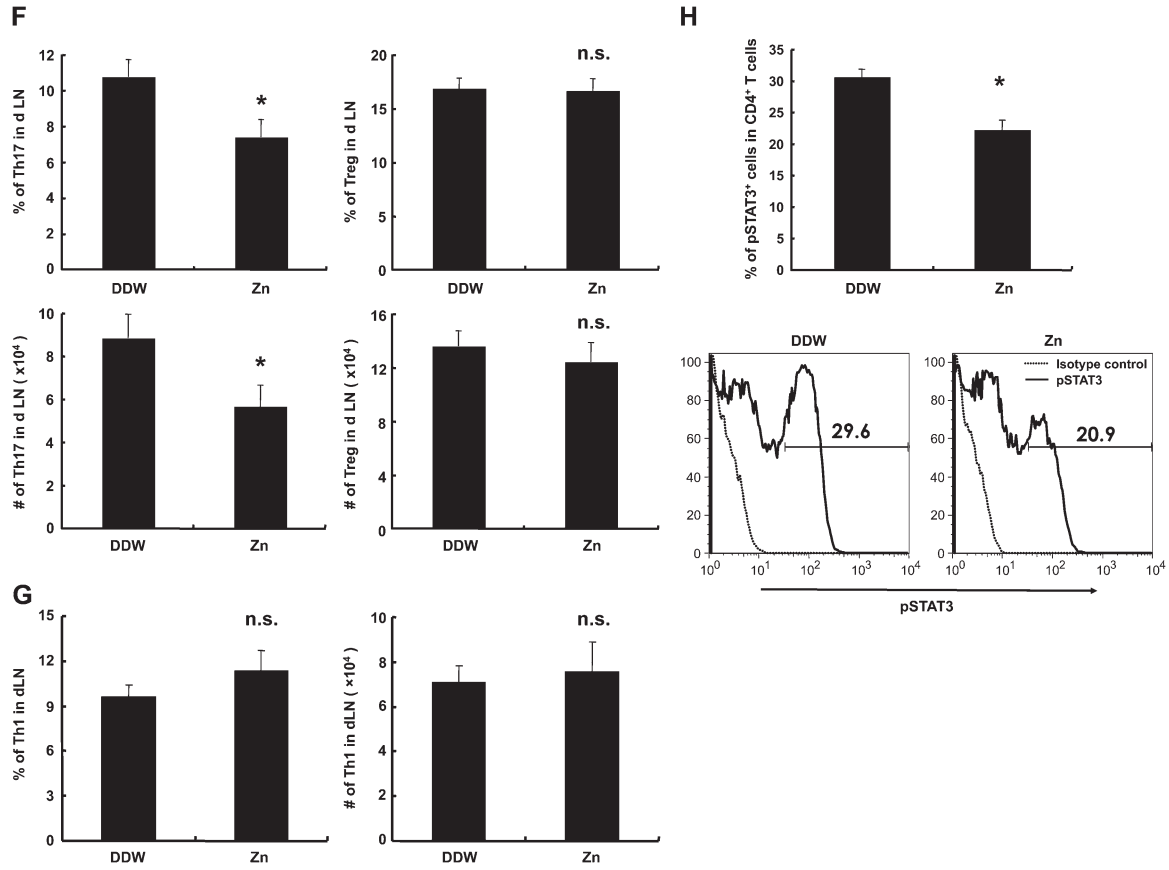

Fig. 1. Continued

cells cultured without IL-6 [average mean fluorescence intensity; 87 for T_h17 plus Zn (n = 3) and 125 for Treg cells (n = 3), see Fig. 2A]. Consistent with lower Foxp3 expression levels, Treg cells cultured in the presence of Zn did not markedly suppress the proliferation of naive $CD4^+$ T cells comparing to normal Treg cells (Supplementary Figure S5 is available at *International Immunology* Online). Thus, the $Foxp3^+$ cells cultured in the presence of Zn were not functionally mature as Treg cells. Importantly, Zn suppressed IL-6-mediated STAT3 activation in $CD4^+$ T cells (Fig. 2B). Conversely, IL-6-mediated JAK phosphorylation did not decrease (Supplementary Figure S6 is available at *International Immunology* Online). All these results demonstrated that Zn inhibits the development of T_h17 cells by suppressing STAT3 activation.

Zn suppresses IL-6-mediated STAT3 activation

To investigate how Zn inhibits IL-6-mediated STAT3 activation, we next examined whether Zn affected the activation states of various proteins in the IL-6-signaling pathway, including STAT3. We employed the RAW246.7 mouse leukemia cell line for this mechanistic analysis because this line is relatively resistant to higher concentrations of intracellular Zn and induced strong IL-6-signaling pathway compared with T cells. We treated these cells with 10 μM $ZnSO_4$ plus pyrithione to allow Zn ions to be efficiently infused into the cells as metal complexes as described previously (15, 36, 37, 50, 51). Zn treatment enhanced IL-6-induced protein phosphorylation (Fig. 3A), consistent with previous reports detailing Zn as an inhibitor of tyrosine phosphatases (52). Zn also enhanced the IL-6-induced activation of JAK proteins and ERK1/2 (Fig. 3A), thereby upregulating the expression of *EGR1*, an ERK1/2 target gene (Supplementary Figure S7 is available at *International Immunology* Online). In contrast, Zn inhibited IL-6-induced tyrosine phosphorylation of STAT3 (Fig. 3A).

The inhibitory effect of Zn on STAT3 activation was also observed in cells stimulated with either IL-10 or LPS (Fig. 3B). Additionally, Zn was shown to inhibit STAT3 functionally, as evidenced by the suppression of IL-6-induced STAT3 nuclear localization in the presence of Zn (Fig. 3C). Furthermore, Zn inhibited IL-6-induced binding of STAT3 to target DNA (Fig. 3D) and the expression of the STAT3 target gene *SOCS3* (Fig. 3E). Therefore, we concluded that Zn inhibits STAT3 activation after IL-6 stimulation without suppressing JAK and ERK activation.

Zn structurally alters STAT3

We then investigated the relationship between Zn and STAT3 using rSTAT3. We found that Zn inhibited STAT3 phosphorylation by both JAK1 and JAK2 without affecting autophosphorylation of these JAK proteins (Fig. 4A). Importantly, Zn did not inhibit the JAK-induced tyrosine phosphorylation of poly-alanine–glutamic acid–lysine–tyrosine peptides

Downloaded from https://academic.oup.com/intimm/article/22/5/375/730670 by guest on 21 October 2022

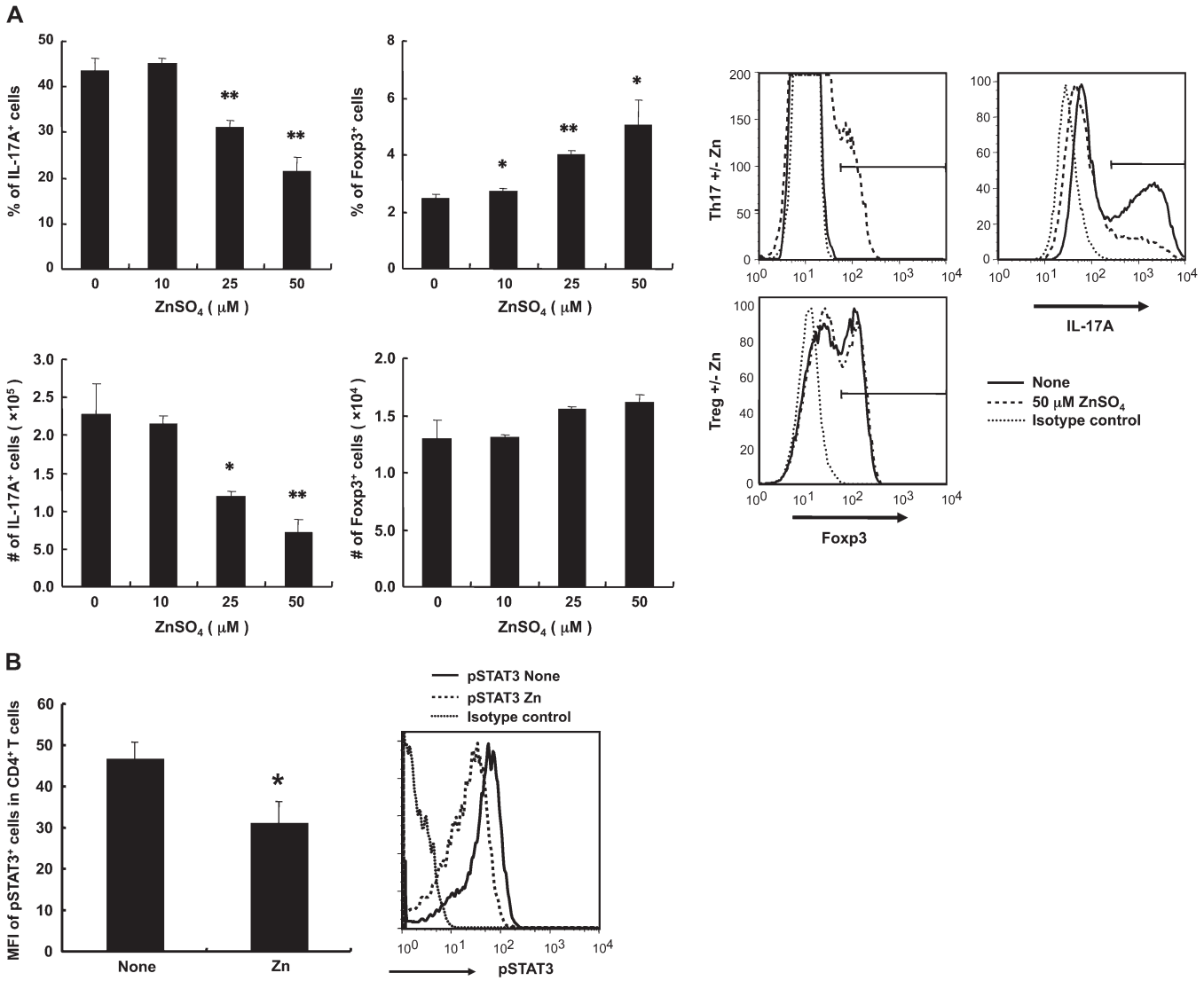

Fig. 2. Zn inhibited the development of T_h17 cells *in vitro*. (A) MoFlo-sorted naive $CD4^+CD44^{lo}$ T cells were stimulated with soluble anti-CD3 antibodies, bone marrow-derived dendritic cells, IL-6 and TGF-β in the presence or absence of $ZnSO_4$ (50 μM). For Treg induction, the naive $CD4^+CD44^{lo}$ T cells were stimulated with soluble anti-CD3 antibodies, bone marrow-derived dendritic cells and TGF-β. Four days later, the cells were labeled intracellularly after stimulation with PMA and ionomycine. The histograms represent IL-17A or Foxp3 expression in $CD4^+$ T cells: the upper left panel shows Foxp3 expression in $CD4^+$ T cells cultured to allow T_h17-cell development (with IL-6) in the presence or absence of Zn. Foxp3 expression was induced in the presence of Zn. The lower left panel shows Foxp3 expression in $CD4^+$ T cells cultured to allow Treg cell development (without IL-6) in the presence or absence of Zn. Foxp3 expression levels under these conditions were higher than those observed in the presence of IL-6 and Zn. The profile for Treg differentiation in the absence of zinc is shown in the lower left panel. The percentage and number of T_h17 cells were lower among Zn-treated $CD4^+$ T cells than among control $CD4^+$ T cells ($P = 0.47$ and 0.64 for 10 μM, $P = 0.0026$ and 0.010 for 25 μM, $P = 0.0008$ and 0.0035 for 50 μM). The percentage of Treg cells was higher among Zn-treated $CD4^+$ T cells than among control $CD4^+$ T cells ($P = 0.04$ for 10 μM, $P = 0.00013$ for 25 μM, $P = 0.032$ for 50 μM). (B) T cells were incubated with 100 μM $ZnSO_4$ for 30 min and stimulated with IL-6 for 5 min. The histograms represent phospho-STAT3 expression in $CD4^+$ T cells. The mean fluorescence intensity (MFI) of the $pSTAT3^+$ cells was significantly lower among the Zn-treated $CD4^+$ T cells than among the control $CD4^+$ T cells ($P = 0.021$). *P* values were calculated using Student's t-test (*$P < 0.05$, **$P < 0.01$).

(poly-AEKY), an artificial substrate for JAK proteins (Fig. 4B). Moreover, STAT3 from cell lysate and rSTAT3 were recovered from IMAC-select beads bearing immobilized Zn (Fig. 4C). These results showed that Zn directly binds STAT3 and inhibits its activation.

We next investigated the effect of Zn binding on the structure of STAT3. Fractionation using native PAGE showed that STAT3 from cells treated with Zn plus pyrithione migrated faster than STAT3 from untreated cells (Fig. 4D, left), an effect that was not observed for α-tubulin (Fig. 4D, right). These results suggested that Zn may change the three-dimensional structure of STAT3 in cells. To study this possibility in more detail, we performed CD spectroscopy, a method used to examine the secondary structures of proteins. The CD spectrum of rSTAT3 showed negative minima at ~222 and 209 nm, which are characteristic of α-helical structures. The addition of Zn reduced the spectral intensity between 200 and 250 nm (Fig. 4E). The Zn chelators EDTA

Downloaded from https://academic.oup.com/intimm/article/22/5/375/730670 by guest on 21 October 2022

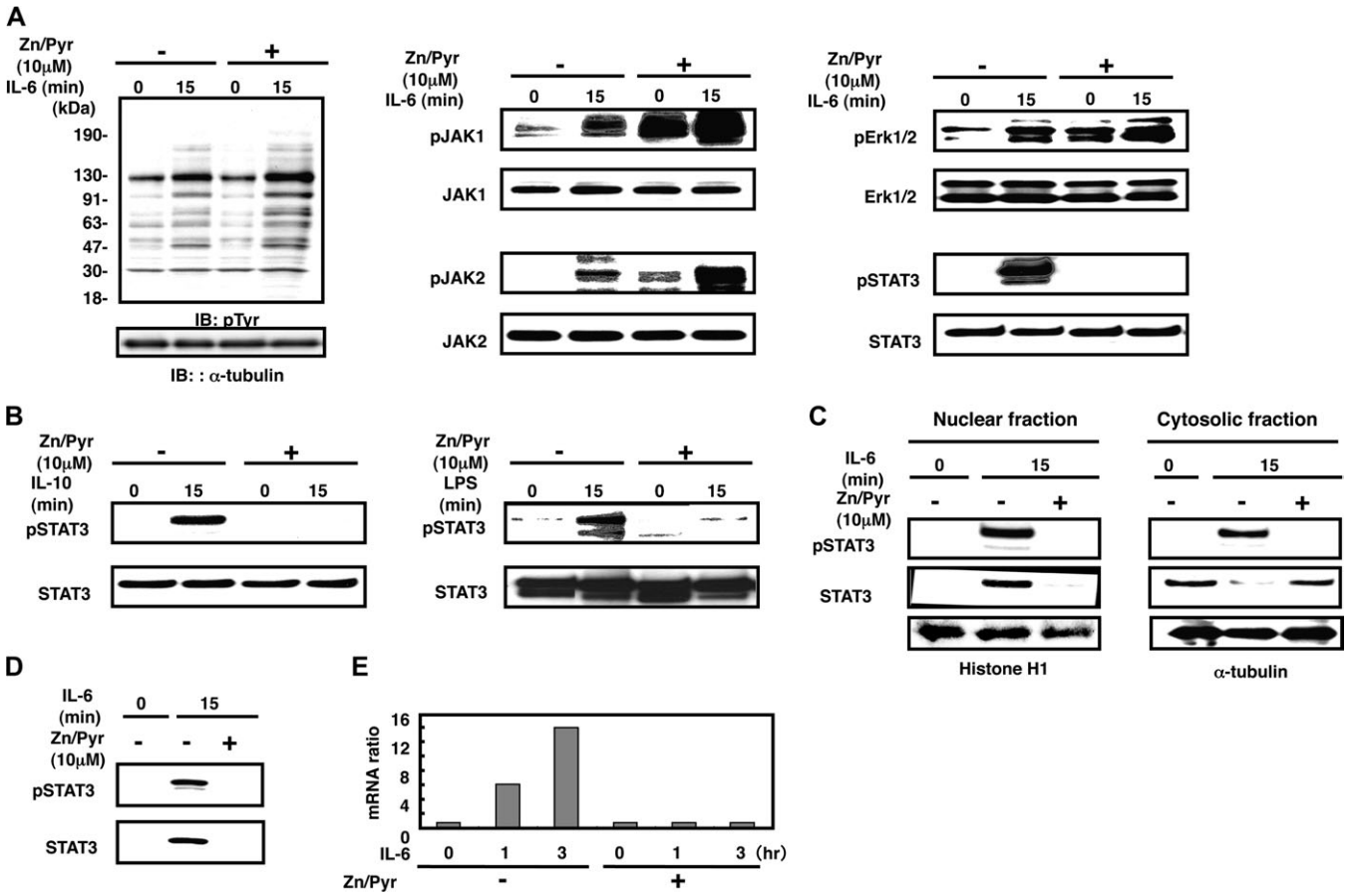

Fig. 3. Zn directly inhibits IL-6-mediated STAT3 activation. (A) RAW246.7 cells were incubated with 10 μM $ZnSO_4$ plus pyrithione for 5 min (Zn/Pyr) and stimulated with IL-6 for 15 min. Total cell lysates or immunoprecipitated samples were subjected to SDS–PAGE followed by immunoblotting with antibodies specific for phospho-tyrosine (pTyr), tyrosyl-phospho (p)-JAK1 (pJAK1), JAK1, pJAK2, JAK2, pERK1/2, ERK1/2, pSTAT3, STAT3 or α-tubulin. (B) After Zn treatment, RAW246.7 cells were stimulated with either IL-10 or LPS. The STAT3-containing immunoprecipitate was immunoblotted with anti-pSTAT3 or anti-STAT3 antibodies. (C) RAW246.7 cells were treated with Zn and stimulated with IL-6 for 15 min. Nuclear (left) and cytosolic (right) fractions were prepared. Each fraction was immunoprecipitated with appropriate anti-STAT3 antibodies and subjected to SDS–PAGE, followed by immunoblotting with anti-pSTAT3, anti-STAT3, anti-histone H1 or anti-α-tubulin antibodies. (D) Nuclear extracts were prepared from Zn-treated RAW246.7 cells and incubated with biotinylated double-stranded DNA probes and streptavidin–Sepharose. The protein–DNA complexes were subjected to SDS–PAGE, followed by immunoblotting with either anti-pSTAT3 or anti-STAT3 antibodies. The probe contained the SBE from the mouse *Socs3* gene. (E) Total RNA was isolated from Zn-treated RAW246.7 cells. Quantitative PCRs were performed with *Socs3*- and *Gapdh*-specific primers.

and TPEN did not restore the intensity in this area of the CD spectrum (Supplementary Figure S8 is available at *International Immunology* Online). These results clearly showed that Zn directly binds to STAT3, which leads to an unfolding of STAT3.

IL-6 binding to its receptor induces the activation of JAK proteins, which in turn results in tyrosine phosphorylation of gp130 (17). STAT3 is then recruited to the tyrosine-phosphorylated YxxQ motif of gp130 through the SH2 domain of STAT3, leading to the tyrosine phosphorylation of STAT3 by JAK proteins. If Zn alters the three-dimensional structure of STAT3, it may inhibit the binding of STAT3 to the tyrosine-phosphorylated YxxQ motif of gp130. Consistent with this hypothesis, Zn inhibited the interaction between a phosphorylated YxxQ peptide and rSTAT3 (Fig. 4F), as well as the *in vitro* binding of rSTAT3 to JAK2 (Fig. 4G). These results demonstrated that structural changes in STAT3 induced by Zn blocked the association of STAT3 with JAK kinase and gp130, both of which are critical for IL-6 signal transduction.

Discussion

We have shown that Zn suppressed CIA development, decreased serum levels of IL-17A but not those of IFN-γ and reduced the numbers of T_h17 cells but not those of T_h1 cells in regional lymph nodes. Importantly, IL-6-induced STAT3 phosphorylation in $CD4^+$ T cells was inhibited by Zn treatment *in vivo*. Moreover, Zn suppressed T_h17 cell development and IL-6-induced STAT3 phosphorylation *in vitro*. Collectively, these results strongly suggested that Zn suppresses T_h17-cell development after the induction of CIA. Mechanistic analysis showed that Zn structurally altered STAT3 to inhibit its activation after IL-6 stimulation. Thus, we conclude that Zn directly suppresses STAT3 activation, which in turn inhibits T_h17-cell development.

Downloaded from https://academic.oup.com/intimm/article/22/5/375/730670 by guest on 21 October 2022

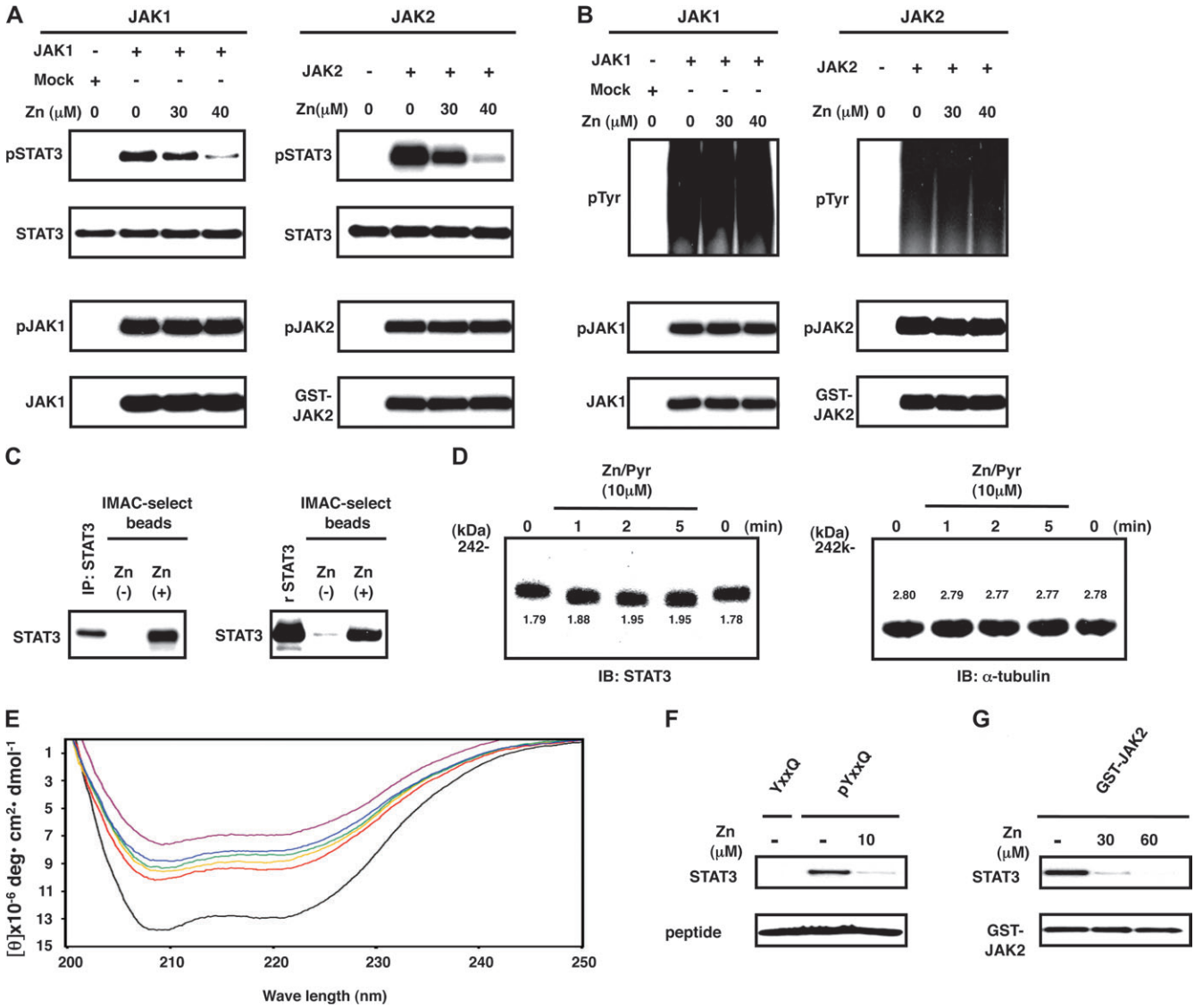

Fig. 4. Zn changes the three-dimensional structure of STAT3. (A) Left: activated JAK1 was used as an rSTAT3 kinase in an *in vitro* reaction. Products were separated by SDS–PAGE and blotted with anti-pSTAT3, anti-STAT3, anti-pJAK1 or anti-JAK1 antibodies. Right: GST-JAK2 was used to phosphorylate rSTAT3 *in vitro*. Reaction products were subjected to SDS–PAGE, followed by immunoblotting with anti-pSTAT3, anti-STAT3, anti-pJAK2 or anti-GST antibodies. (B) Poly-AEKY was used as the substrate in an *in vitro* kinase reaction with either JAK1 (left) or GST-JAK2 (right). The products were subjected to SDS–PAGE followed by immunoblotting with the indicated antibodies. (C) Zn immobilized on IMAC-select affinity beads was incubated with 100 μg of RAW246.7 cell lysate (left) or 0.1 μg of rSTAT3 (right). The beads were washed, subjected to SDS–PAGE and blotted with anti-STAT3 antibodies. (D) RAW246.7 cells were treated with Zn for the indicated periods of time. Cell lysates were separated by native PAGE and immunoblotted with anti-STAT3 (left) or anti-α-tubulin (right) antibodies. The migration distance (cm) from the 242-kDa molecular weight marker is given below the bands in the gel images. (E) The graph shows CD spectra of STAT3 in the absence (black) or presence of Zn (red, 1 μM; yellow, 5 μM; green, 10 μM; blue, 50 μM and magenta, 150 μM). (F) A gp130 peptide-binding assay performed using rSTAT3 and Zn treatment. (G) A GST-JAK2-binding assay performed with rSTAT3.

Zinc is an essential nutrient to maintain normal physiological functions *in vivo*. But excess Zn ions are thought to be toxic. However, as shown in Supplementary Figure S2 (available at *International Immunology* Online), administering 3000 p.p.m. Zn for 2 months did not alter the sizes of various lymph node and spleen immune cell populations. In fact, serum Zn concentration in mice having a drinking water with 3000 p.p.m. of Zn is ~30 μM, while control mice contained ~15 μM of Zn in serum (Supplementary Figure S3 is available at *International Immunology* Online). This concentration of Zn is much lower than those reported to be toxic and may not in fact promote T-cell death based on *in vitro* experiments (Supplementary Figure S4 is available at *International Immunology* Online). Importantly, body weight of the mice having 3000 p.p.m. Zn was not changed comparing to that of control animals (data not shown). Moreover, autoimmune diseases induced by pathogenic T-cell transfer developed normally in mice receiving 3000 p.p.m. Zn in drinking water (Fig. 1C). These results demonstrated that 3000 p.p.m. Zn in drinking water did not completely disrupt immune responses in mice.

Downloaded from https://academic.oup.com/intimm/article/22/5/375/730670 by guest on 21 October 2022

We used 50 μM Zn for the *in vitro* T_h17-cell differentiation experiments. We wanted to investigate the effects of Zn in an experimental system that mimicked physiologic conditions. Intracellular Zn concentrations are mainly regulated *in vivo* by Zn transporters. For experiments with primary T cells, we used Zn alone rather than complexes of Zn and pyrithione because Zn enters cells via transporters under physiologic conditions, whereas complexes of Zn and pyrithione enter cells with or without functioning Zn transporters. After 4 days of culture to induce T_h17-cell development, the primary T cells were viable in culture medium containing <120 μM Zn, whereas T_h17-cells development was suppressed in medium containing >25 μM Zn (Fig. 2A). Moreover, we showed that mice having 3000 p.p.m. of Zn in a drinking water showed ~30 μM Zn in their sera (Supplementary Figure S3 is available at *International Immunology* Online). Therefore, we used medium containing 50 μM Zn for this assay to obtain robust data without markedly affecting cell survival.

On the other hand, for the mechanistic analysis, several reports have described the effects of Zn on various cell lines, including biochemical studies of signal transduction using Zn plus pyrithione (15, 36, 37, 50, 51). The concentrations of Zn and pyrithione in these studies ranged from 4 to 20 μM. An advantage of Zn plus pyrithione treatment is that complexes of Zn ions and pyrithione enter cells rapidly and directly through the plasma membrane rather than Zn transporters. Rapid infusion of Zn is important when investigating molecules in signaling cascades that are rapidly activated, such as the IL-6-signaling pathway. Thus, we treated the cell lines with 10 μM $ZnSO_4$ plus pyrithione. Using this method, we showed that Zn suppressed STAT3 activation in the IL-6-signaling pathway. These results are consistent with data obtained using more physiologic Zn infusion methods, which resulted in decreased numbers of T_h17 cells *in vivo* without affecting the Treg cell population during the induction of CIA. Moreover, *in vitro* experiments similarly demonstrated a decreased number of T_h17 cells, whereas the functional Treg cell number did not increase after Zn administration. Importantly, IL-6-mediated STAT3 activation was significantly inhibited in both cases. Taken together, these results support the idea that Zn directly suppresses STAT3 activation, a critical step during T_h17-cell development.

Although we showed that Zn suppresses STAT3 activation, it is unclear whether Zn selectively affects STAT3 but not other STAT family members. We showed that *in vivo* Zn treatment reduced the number of T_h17 cells without significantly affecting T_h1 cells. Consistent with this result, the Zn-mediated suppressive effects were more evident in cultures of developing T_h17 cells compared with those of T_h1 cells (Supplementary Figure S9 is available at *International Immunology* Online). Together with *in vivo* results shown in Fig. 1, these results suggested that Zn affects T_h17 cells more than T_h1 cells. It should be pointed out, however, that forced infusion of Zn using pyrithione suppressed the phosphorylation of a variety of STAT molecules, including STAT1, STAT4 and STAT5 (Supplementary Figure S10 is available at *International Immunology* Online). One potential explanation for this discrepancy is that expression profiles of Zn transporters and/or Zn-binding proteins may differ in T_h1 and T_h17 cells. Zn may affect only STAT3 in T_h17 cells under physiological conditions, whereas forced infusion of Zn *in vitro* suppresses a broad range of STAT molecules in various cell types. Consistent with this notion, we observed that expression profiles of some Zn transporters are differ between T_h1 and T_h17 cells (Supplementary Figure S11 is available at *International Immunology* Online). Therefore, zinc-mediated STAT3 regulation might be a nice way to control many inflammatory diseases including autoimmune diseases where STAT3 is involved in their pathogenesis.

It is important to know whether Zn-mediated suppression of STAT3 activation is induced in physiological conditions. We hypothesize that Zn-mediated STAT3 suppression works as one of intracellular STAT3 regulations. Consistent with this, mRNA expressions of Zn transporters are changed by various extrinsic stimulations, some of which are known to induce STAT3 activation in organs and cells, including T cells (53–56). Of note, a data showed that T_h17 cells induced a decrease in the intensity for fluorescent of Zn indicators, Newport green, comparing to naive $CD4^+$ T cells (Supplementary Figure S12 is available at *International Immunology* Online), suggesting that a lower Zn concentration in T_h17 cells might enhance the development of this population. However, it should be pointed out that CIA developed similarly in B6 mice receiving a Zn-deficient diet (<0.3 mg 100 g^{-1}) or a control normal diet (3 mg 100 g^{-1}) for >1 month (Supplementary Figure S13 is available at *International Immunology* Online). We showed that the serum Zn concentration decreased by ~10% in mice receiving the Zn-deficient diet. Although it has been suggested that a Zn-deficient diet suppresses T-cell activation (57), the 10% reduction in serum Zn levels may not have affected immune responses *in vivo*, whereas a 2-fold increase in serum Zn (29 μM Zn in mice receiving 3000 p.p.m. Zn in their drinking water) significantly altered the T-cell responses. Diets with less Zn can only be used under carefully controlled conditions, however. Further studies are needed to examine the effects of Zn deficiency on *in vivo* T-cell responses.

Another important question is whether Zn administration affects more T_h17-cell differentiation comparing to other cell populations including non-T cells because Zn may play roles for regulating many biological phenomena in a number of cell populations especially *in vivo*. Moreover, it might be possible that the inhibitory effect of Zn on T_h17 differentiation is due to the Foxp3 inducing activity of Zn because Foxp3 expression is inhibitory to T_h17 differentiation. Presently, however, we have hypothesized that the induction of Foxp3 expression by Zn does not contribute to the Zn-mediated suppression of T_h17 cell development because 25 μM Zn suppressed the differentiation of T_h17 cells, but this concentration of Zn did not increase the numbers of Treg cells (Fig. 2A).

The structure of STAT3 was altered after Zn binding. Structural changes in rSTAT3 were detected using two methods in the presence or absence of Zn: native PAGE and CD spectroscopy. The Zn-induced changes in STAT3 may block a primary component of IL-6 signaling, i.e. STAT3 activation. Consistent with this idea, IL-6-mediated STAT3 nuclear localization and its transcriptional activity were inhibited by Zn treatment. Moreover, Zn-bound STAT3 did not associate with

Downloaded from https://academic.oup.com/intimm/article/22/5/375/730670 by guest on 21 October 2022

JAK1 or a gp130 fragment bearing a phosphorylated tyrosine residue essential for STAT3 binding; each of these binding events is critical for IL-6-mediated STAT3 activation to induce the development of T_h17 cells. Thus, it is possible that STAT3 might be a target of Zn signaling in T cells.

In summary, we have shown that Zn directly suppresses STAT3 activation, which is a critical step in T_h17-cell development followed by autoimmune disease development.

Supplementary data

Supplementary Figures S1–S13 are available at *International Immunology* Online.

Funding

KAKENHI to C.K., M.M. and T.H.; Core Research for Evolutional Science and Technology to M.M. and T.H.; Uehara Foundation to M.M.; Osaka Foundation for the Promotion of Clinical Immunology to M.M. and T.H.

Acknowledgements

We thank Dr Bernard Malissen (Université de la Méditerranée, Marseille, France) for the Foxp3-GFP reporter mice (58). We appreciate the excellent technical assistance provided by Ms Jiang, Ms Sato, Ms Iketani, Ms Asanuma, Ms Itoh, Mr Kawamura and Ms Hayashi and thank Ms Masuda and Ms Shimura for their excellent secretarial assistance. We thank Dr Kamimura for carefully reading this manuscript.
Conflict of Interest: The authors declare that they have no conflicting financial interests.

References

1 Kambe, T., Weaver, B. P. and Andrews, G. K. 2008. The genetics of essential metal homeostasis during development. *Genesis* 46:214.
2 Vallee, B. L. and Auld, D. S. 1993. Cocatalytic zinc motifs in enzyme catalysis. *Proc. Natl Acad. Sci. USA* 90:2715.
3 Prasad, A. S. 1995. Zinc: an overview. *Nutrition* 11:93.
4 Brown, H., Peerson, J. M., Allen, L. H. and Rivera, J. 2002. Effect of supplemental zinc on the growth and serum zinc concentrations of pre-pubertal children: a meta-analysis of randomized, controlled trials. *Am. J. Clin. Nutr.* 75:1062.
5 Wellinghausen, N., Kirchner, H. and Rink, L. 1997. The immunobiology of zinc. *Immunol. Today* 18:519.
6 Ibs, K. H. and Rink, L. 2003. Zinc-altered immune function. *J. Nutr.* 133:1452S.
7 King, L. E., Osati-Ashtiani, F. and Fraker, P. J. 2002. Apoptosis plays a distinct role in the loss of precursor lymphocytes during zinc deficiency in mice. *J. Nutr.* 132:974.
8 Prasad, A. S. 2000. Effects of zinc deficiency on Th1 and Th2 cytokine shifts. *J. Infect. Dis.* 182 (Suppl. 1):S62.
9 Bhutta, Z. A., Bird, S. M., Black, R. E. *et al.* 2000. Therapeutic effects of oral zinc in acute and persistent diarrhea in children in developing countries: pooled analysis of randomized controlled trials. *Am. J. Clin. Nutr.* 72:1516.
10 Fraker, P. J., King, L. E., Laakko, T. and Vollmer, T. L. 2000. The dynamic link between the integrity of the immune system and zinc status. *J. Nutr.* 130:1399S.
11 Tran, C. D., Ball, J. M., Sundar, S., Coyle, P. and Howarth, G. S. 2007. The role of zinc and metallothionein in the dextran sulfate sodium-induced colitis mouse model. *Dig. Dis. Sci.* 52:2113.
12 Ohkawara, T., Takeda, H., Kato, K. *et al.* 2005. Polaprezinc (N-(3-aminopropionyl)-L-histidinato zinc) ameliorates dextran sulfate sodium-induced colitis in mice. *Scand. J. Gastroenterol.* 40:1321.
13 Ohly, P., Dohle, C., Abel, J., Seissler, J. and Gleichmann, H. 2000. Zinc sulphate induces metallothionein in pancreatic islets of mice and protects against diabetes induced by multiple low doses of streptozotocin. *Diabetologia* 43:1020.
14 Yamashita, S., Miyagi, C., Fukada, T., Kagara, N., Che, Y. S. and Hirano, T. 2004. Zinc transporter LIVI controls epithelial-mesenchymal transition in zebrafish gastrula organizer. *Nature* 429:298.
15 Kitamura, H., Morikawa, H., Kamon, H. *et al.* 2006. Toll-like receptor-mediated regulation of zinc homeostasis influences dendritic cell function. *Nat. Immunol.* 7:971.
16 Liuzzi, J. P., Aydemir, F., Nam, H., Knutson, M. D. and Cousins, R. J. 2006. Zip14 (Slc39a14) mediates non-transferrin-bound iron uptake into cells. *Proc. Natl Acad. Sci. USA* 103:13612.
17 Hirano, T. 1998. Interleukin 6 and its receptor: ten years later. *Int. Rev. Immunol.* 16:249.
18 Bettelli, E., Oukka, M. and Kuchroo, V. K. 2007. T(H)-17 cells in the circle of immunity and autoimmunity. *Nat. Immunol.* 8:345.
19 Nishihara, M., Ogura, H., Ueda, N. *et al.* 2007. IL-6-gp130-STAT3 in T cells directs the development of IL-17+ Th with a minimum effect on that of Treg in the steady state. *Int. Immunol.* 19:695.
20 Ivanov, I. I., McKenzie, B. S., Zhou, L. *et al.* 2006. The orphan nuclear receptor RORgammat directs the differentiation program of proinflammatory IL-17+ T helper cells. *Cell* 126:1121.
21 Veldhoen, M., Hocking, R., Atkins, C., Locksley, R. and Stockinger, B. 2006. TGF in the context of an inflammatory cytokine milieu supports *de novo* differentiation of IL-17-producing T cells. *Immunity* 24:179.
22 Darnell, J. E., Jr. 1997. STATs and gene regulation. *Science* 277:1650.
23 Yasukawa, H., Sasaki, A. and Yoshimura, A. 2000. Negative regulation of cytokine signaling pathways. *Annu. Rev. Immunol.* 18:143.
24 Mosmann, T. R. and Coffman, R. L. 1989. TH1 and TH2 cells: different patterns of lymphokine secretion lead to different functional properties. *Annu. Rev. Immunol.* 7:145.
25 Glimcher, L. H. and Murphy, K. M. 2000. Lineage commitment in the immune system: the T helper lymphocyte grows up. *Genes Dev.* 14:1693.
26 Zhu, J., Yamane, H., Cote-Sierra, J., Guo, L. and Paul, W. E. 2006. GATA-3 promotes Th2 responses through three different mechanisms: induction of Th2 cytokine production, selective growth of Th2 cells and inhibition of Th1 cell-specific factors. *Cell Res.* 16:3.
27 Cua, D. J., Sherlock, J., Chen, Y. *et al.* 2003. Interleukin-23 rather than interleukin-12 is the critical cytokine for autoimmune inflammation of the brain. *Nature* 421:744.
28 Harrington, L. E., Hatton, R. D., Mangan, P. R. *et al.* 2005. Interleukin 17-producing CD4+ effector T cells develop via a lineage distinct from the T helper type 1 and 2 lineages. *Nat. Immunol.* 6:1123.
29 Park, H., Li, Z., Yang, X. O. *et al.* 2005. A distinct lineage of CD4 T cells regulates tissue inflammation by producing interleukin 17. *Nat. Immunol.* 6:1133.
30 Ogura, H., Murakami, M., Okuyama, Y. *et al.* 2008. Interleukin-17 promotes autoimmunity by triggering a positive-feedback loop via interleukin-6 induction. *Immunity.* 29:628.
31 Afzali, B., Lombardi, G., Lechler, R. I. and Lord, G. M. 2007. The role of T helper 17 (Th17) and regulatory T cells (Treg) in human organ transplantation and autoimmune disease. *Clin. Exp. Immunol.* 148:32.
32 Iwakura, Y. and Ishigame, H. 2006. The IL-23/IL-17 axis in inflammation. *J. Clin. Invest.* 116:1218.
33 Hirota, K., Hashimoto, M., Yoshitomi, H. *et al.* 2007. T cell self-reactivity forms a cytokine milieu for spontaneous development of IL-17+ Th cells that cause autoimmune arthritis. *J. Exp. Med.* 204:41.
34 Hirano, T., Murakami, M., Fukada, T., Nishida, K., Yamasaki, S. and Suzuki, T. 2008. Roles of zinc and zinc signaling in immunity: zinc as an intracellular signaling molecule. *Adv. Immunol.* 97:149.
35 Hogstrand, C., Kille, P., Nicholson, R. I. and Taylor, K. M. 2009. Zinc transporters and cancer: a potential role for ZIP7 as a hub for tyrosine kinase activation. *Trends Mol. Med.* 15:101.
36 Haase, H., Ober-Blöbaum, J. L., Engelhardt, G. *et al.* 2008. Zinc signals are essential for lipopolysaccharide-induced signal transduction in monocytes. *J. Immunol.* 181:6491.

Downloaded from https://academic.oup.com/intimm/article/22/5/375/730670 by guest on 21 October 2022

37 Yamasaki, S., Sakata-Sogawa, K., Hasegawa, A. *et al.* 2007. Zinc is a novel intracellular second messenger. *J. Cell Biol.* 177:637.
38 Nishida, K., Hasegawa, A., Nakae, S., Oboki, K., Saito, H. and Yamasaki, S. T. H. 2009. Zinc transporter Znt5/Slc30a5 is required for the mast cell-mediated delayed-type allergic reaction but not the immediate-type reaction. *J. Exp. Med.* 206:1351.
39 Fukada, T., Civic, N., Furuichi, T. *et al.* 2008. The zinc transporter SLC39A13/ZIP13 is required for connective tissue development; its involvement in BMP/TGF-beta signaling pathways. *PLoS ONE* 3:e3642.
40 Bruinsma, J. J., Jirakulaporn, T., Muslin, A. J. and Kornfeld, K. 2002. Zinc ions and cation diffusion facilitator proteins regulate Ras-mediated signaling. *Dev. Cell* 2:567.
41 Nakae, S., Nambu, A., Sudo, K. and Iwakura, Y. 2003. Suppression of immune induction of collagen-induced arthritis in IL-17-deficient mice. *J. Immunol.* 171:6173.
42 Ogura, H., Murakami, M., Okuyama, Y. *et al.* 2008. Dysregulation of an IL-17-triggered positive feedback loop of IL-6 signaling in an autoimmune arthritis. *Immunity* 29:628.
43 Takahashi-Tezuka, M., Yoshida, Y., Fukada, T. *et al.* 1998. Gab1 acts as an adapter molecule linking the cytokine receptor gp130 to ERK mitogen-activated protein kinase. *Mol. Cell Biol.* 18: 4109.
44 Fukada, T. and Tonks, N. K. 2001. The reciprocal role of Egr-1 and Sp family proteins in regulation of the PTP1B promoter in response to the p210 Bcr-Abl oncoprotein-tyrosine kinase. *J. Biol. Chem.* 276:25512.
45 Gatto, L., Berlato, C., Poli, V. *et al.* 2004. Analysis of SOCS-3 promoter responses to interferon gamma. *J. Biol. Chem.* 279:13746.
46 Sasai, M., Saeki, Y., Ohshima, S. *et al.* 1999. Delayed onset and reduced severity of collagen-induced arthritis in interleukin-6-deficient mice. *Arthritis Rheum.* 42:1635.
47 Turgut, G., Abban, G., Turgut, S. and Take, G. 2003. Effect of overdose zinc on mouse testis and its relation with sperm count and motility. *Biol. Trace Elem. Res.* 96:271.
48 Groeneveld, G. J., de Leeuw van Weenen, J., van Muiswinkel, F. L. *et al.* 2003. Zinc amplifies mSOD1-mediated toxicity in a transgenic mouse model of amyotrophic lateral sclerosis. *Neurosci. Lett.* 352:175.
49 Gaworski, C. L. and Sharma, R. P. 1978. The effects of heavy metals on [3H]thymidine uptake in lymphocytes. *Toxicol. Appl. Pharmacol.* 46:305–313.
50 Uzzo, R. G., Leavis, P., Hatch, W. *et al.* 2002. Zinc inhibits nuclear factor-kappa B activation and sensitizes prostate cancer cells to cytotoxic agents. *Clin. Cancer Res.* 8:3579.
51 Kojima, C., Kawakami, A., Takei, T., Nitta, K. and Yoshida, M. 2007. Angiotensin-converting enzyme inhibitor attenuates monocyte adhesion to vascular endothelium through modulation of intracellular zinc. *J. Pharmacol. Exp. Ther.* 323:855.
52 Haase, H. and Maret, W. 2005. Protein tyrosine phosphatases as targets of the combined insulinomimetic effects of zinc and oxidants. *Biometals* 18:333–338.
53 Aydemir, T. B., Liuzzi, J. P., McClellan, S. and Cousins, R. J. 2009. Zinc transporter ZIP8 (SLC39A8) and zinc influence IFN-gamma expression in activated human T cells. *J. Leukoc. Biol.* 86:337.
54 Lang, C., Murgia, C., Leong, M. *et al.* 2007. Anti-inflammatory effects of zinc and alterations in zinc transporter mRNA in mouse models of allergic inflammation. *Am. J. Physiol. Lung Cell. Mol. Physiol.* 292:L577.
55 Liuzzi, J. P., Lichten, L. A., Rivera, S. *et al.* 2005. Interleukin-6 regulates the zinc transporter Zip14 in liver and contributes to the hypozincemia of the acute-phase response. *Proc. Natl Acad. Sci. USA* 102:6843.
56 Bury, N. R., Chung, M. J., Sturm, A., Walker, P. A. and Hogstrand, C. 2008. Cortisol stimulates the zinc signaling pathway and expression of metallothioneins and ZnT1 in rainbow trout gill epithelial cells. *Am. J. Physiol. Regul. Integr. Comp. Physiol.* 294:R623.
57 Hönscheid, A., Rink, L. and Haase, H. 2009. T-lymphocytes: a target for stimulatory and inhibitory effects of zinc ions. *Endocr. Metab. Immune Disord. Drug Targets* 9:132.
58 Wang, Y., Kissenpfennig, A., Mingueneau, M. *et al.* 2008. Th2 lymphoproliferative disorder of LatY136F mutant mice unfolds independently of TCR-MHC engagement and is insensitive to the action of Foxp3+ regulatory T cells. *J. Immunol.* 180:1565.

Downloaded from https://academic.oup.com/intimm/article/22/5/375/730670 by guest on 21 October 2022